Approximate Cramér-Rao bound on Doppler error in correlation-processing relatively narrowband noise radar *

Michał Meller

Telecommunications Research Institute Gdansk Division

Department of Signal and Information Processing

Hallera 233A, 80-502 Gdańsk, Poland

e-mail: michal.meller@pit.gda.pl

October 7, 2008

Abstract

The paper studies limitations on accuracy of Doppler estimation in continuous-wave noise radar with correlation processing. Second order properties of output of the correlation receiver are evaluated and an approximate Cramér-Rao bound on errors of Doppler measurement is derived. The accuracy of Doppler measurements is found to be affected by the following factors: power spectral density of noise signal, frequency response of the lowpass filter in correlator, observation time, velocity of the target and signal to noise ratio. It is shown that the random nature of the transmitted signal induces additional fluctuations at the output of correlator which limit the accuracy even in the infinite signal to noise case. Qualitative extension of the results to a case covering multiple targets and clutter is made. It is argued that the performance will decrease and that increasing transmitted power may not provide significant improvement when clutter is present.

Index terms—correlation, Doppler, estimation, noise radar, radar theory

*This work was supported by the National Center for Research and Development for the years 2007-2010 under Commissioned Research Project PBZ-MNiSW-DBO-04/I/2007

1 Introduction

Noise radars use truly random signals, a class of signals which offers some strong advantages, namely: nearly ideal 'thumbtack' ambiguity function, unambiguity in both range and Doppler[1, 2, 3], low probability of intercept, and high immunity agains jamming and interference [4].

Since the signal is unknown until its generation, special processing techniques must be used in noise radars. Probably the most common one is correlation processing[1, 5, 2]. The received signal is cross-correlated with the delayed replica of the transmitted signal to provide an estimate of reflectivity at a range corresponding to a given time-delay. The importance of this approach stems from the fact that it is equivalent to a matched filter. In pulsed radars, each output sample of the matched filter can easily be shown to equal the correlation sum of the appropriately delayed pulse and the received signal. Since however, the noise signal is unpredictable, one cannot implement matched filter as typical time-invariant filter and must use a bank of correlators – each 'matched' to a different delay.

This technique has its limitations, however. From the practical viewpoint, the most important is that correlation result always contains some residual fluctuations. Most vaguely speaking, even in point scatterer and infinite signal-to-noise ratio scenario, the result of correlation processing will be nonzero at all range cells. Some efforts to cope with this issue has been made by Kulpa[6, 7], Axelsson[8] and Narayanan and coworkers[9].

This paper studies the limitations of correlation processing in Doppler estimation. The ability of noise radar to estimate the Doppler was demonstrated by Narayanan and coworkers[10, 11, 12]. In [10] some qualitative remarks are made on the possible accuracy. In [12] the empirical phase-noise model was developed. The aim of this paper is to extend results from mentioned papers by providing both quantitative and qualitative results. First, we derive the expressions for the power spectral density of the stochastic part of correlation receiver output. This in turn, allows to derive approximate Cramér-Rao bound on the accuracy of Doppler processing. Both results were obtained in a point scatterer scenario. Additionally, a short discussion is made on the extension to a more realistic multiple scatterer case. It is found that in such case the performance of noise radar with correlation processing will inevitably deteriorate.

The paper is organised as follows: section 2 presents the mathematical model of the noise radar system. In section 3 spectral analysis of signals in system for the point scatterer case is performed. In section 4 Cramér-Rao bound is derived. Section 5 concludes.

2 Mathematical model of radar system

A block diagram of a mathematical model of a coherent continuous wave noise radar with correlation processing is shown in Fig. 1

A stochastic process $x(t)$ is generated in a noise source NS and divided into two paths: the transmit antenna path and the reference path. The reference signal is delayed in a delay line DL by the amount D.

The received signal, $y(t)$ - contaminated by the noise $n(t)$ - is multiplied with the reference in a mixer MIX. The product of multiplication $c_D(t)$ (further called 'raw product' since this signal is very noisy) is lowpass-filtered in a filter with frequency response $G(j\omega)$ to form a smoothed correlation signal $\tilde{c}_D(t)$. The latter is sampled with sampling frequency $1/T_s$ to form the discrete-time signal $\tilde{c}_D(n) = \tilde{c}_D(nT_s)$ which is then digitally Doppler processed.

Let us now form basic assumption about the signals $x(t)$ and $n(t)$ in the system:

(A1) $x(t)$ and $n(t)$ are zero-mean, wide-sense stationary circular complex Gaussian[1] stochastic processes with correlation function

$$\mathbf{R}(\tau) = \mathrm{E}\left[\begin{array}{c} x(t) \\ n(t) \end{array}\right]\left[\begin{array}{cc} x(t-\tau) & n(t-\tau) \end{array}\right]^* = \\ = \left[\begin{array}{cc} R_{xx}(\tau) & 0 \\ 0 & R_{nn}(\tau) \end{array}\right] \tag{1}$$

where * denotes complex conjugation. The power spectral density

$$\mathbf{S}(\omega) = \mathscr{F}[\mathbf{R}(\tau)] = \left[\begin{array}{cc} S_{xx}(\omega) & 0 \\ 0 & S_{nn}(\omega) \end{array}\right] \tag{2}$$

is focused around angular frequency ω_0.

Remark

The assumption of the signals in system being complex simplifies the discussion considerably. However, the results obtained here are also valid for the real signals. This stems from the fact that, for any real signal, it's complex equivalent can be found using Hilbert transform. Such Hilbert-transformed signal satisfies (A1)

[1] The term circular means that the real and imaginary part are jointly Gaussian, independent, and have equal variance.

and carries exactly the same amount of information as the original real signal. It follows that bounds on Doppler error of these two signals are equal.

3 Signal properties

In this section, second order properties of the correlator output will be analysed. Before we proceed further, let us introduce natural assumption

(**A2**) The target is moving with radial velocity $v \ll c$. It is assumed that v is positive when the Doppler shift is also positive, i.e. the target is closing towards the radar.

Also assume

(**A3**) The process $x(t)$ is *relatively* narrowband, i.e. its bandwidth B satisfies $B \ll F_0$

Some remarks about (A3) are given at the end of the section.

Under (A2)-(A3) the received signal can be written as

$$y(t) = Fx(t - \tau(t)) + n(t) \tag{3}$$

where F is complex reflection coefficient and

$$\tau(t) \cong \tau(0) - \frac{2v}{c}t = 2\frac{R_0 - vt}{c}$$

is the two-way propagation delay.

3.1 First and second order properties of the raw product signal

Consider now the value of the raw product

$$c_D(t) = y(t)x^*(t - D) \ .$$

By analysing first and second order properties of this signal, we will be able to guess on the properties of the smoothed correlation signal using basic results from linear filtration theory.

One can perform decomposition into deterministic and stochastic part

$$c_D(t) = \mathrm{E}[c_D(t)] + (c_D(t) - \mathrm{E}[c_D(t)]) = \mathrm{E}[c_D(t)] + w(t)$$

The expectation is purely deterministic, while $w(t)$ represents the random fluctuations of $c_D(t)$. It is straightforward to check that [12]

$$\mathrm{E}[c_D(t)] = FR_{xx}(D - \tau(t)) = FR_{xx}(D - \tau(0) + \beta t) \tag{4}$$

where $\beta = 2v/c$. Also note that for $D = \tau(0)$ [12]

$$\mathscr{F}\mathrm{E}[c_D(t)] = \frac{F}{\beta} S_{xx}(\frac{\omega}{\beta}). \tag{5}$$

This means that the deterministic part is localized in the frequency domain around angular frequency $\omega_0\beta$.

We now move on to the calculation of correlation function and power spectral density of the stochastic part $w(t)$. The correlation function of $w(t)$ (which is also the covariance function of $c_D(t)$) is

$$\begin{aligned} R_{ww}(t,s) &= \mathrm{E}[w(t)w^*(s)] = \\ &= \mathrm{E}[(c_D(t) - E[c_D(t)])\times \\ &\qquad \times (c_D(s) - E[c_D(s)])^*] = \\ &= \mathrm{E}[c_D(t)c_D^*(s)] - E[c_D(t)]E[c_D^*(s)] = \\ &= I_1 - I_2 \end{aligned} \tag{6}$$

Evaluation of I_2 is trivial

$$I_2 = |F|^2 R_{xx}(D - \tau(t))R_{xx}^*(D - \tau(s)).$$

I_1 is sum of four components

$$I_1 = I_{1,1} + I_{1,2} + I_{1,3} + I_{1,4}$$

where

$$I_{1,1} = \mathrm{E}[|F|^2 x(t-\tau(t))x^*(t-D)\times$$
$$\times\, x(s-D)x^*(s-\tau(s))]$$
$$I_{1,2} = \mathrm{E}[Fx(t-\tau(t))x^*(t-D)n(s)x(s-D)]$$
$$I_{1,3} = \mathrm{E}[F^* n(t)x(t-D)x^*(s-\tau(s))x(s-D)]$$
$$I_{1,4} = \mathrm{E}[n(t)n^*(s)x(s-D)x^*(t-D)]$$

From (A1) it immediately follows that

$$I_{1,2} = 0$$
$$I_{1,3} = 0$$
$$I_{1,4} = R_{nn}(t-s)R_{xx}(s-t)$$

and $I_{1,1}$ can be further decomposed into [13]

$$I_{1,1} = |F|^2(I_{1,1,1} + I_{1,1,2} + I_{1,1,3})$$

where

$$I_{1,1,1} = \mathrm{E}[x(t-\tau(t))x^*(t-D)]\times$$
$$\times\ \mathrm{E}[x(s-D)x^*(s-\tau(s))] =$$
$$= R_{xx}(D-\tau(t))R^*_{xx}(D-\tau(s))$$
$$I_{1,1,2} = \mathrm{E}[x(t-\tau(t))x^*(s-\tau(s))]\times$$
$$\times\ \mathrm{E}[x^*(t-D)x(s-D)] =$$
$$= R_{xx}(t-s+\tau(s)-\tau(t))R_{xx}(s-t)$$
$$I_{1,1,3} = \mathrm{E}[x(t-\tau(t))x(s-D)]\times$$
$$\times\ \mathrm{E}[x^*(t-D)x^*(s-\tau(s))] =$$
$$= 0$$

and the last equality stems from circularity of $x(t)$.

Putting all together, one obtains

$$\begin{aligned} R_{ww}(t,s) &= |F|^2 R_{xx}(t-s+\tau(s)-\tau(t))R_{xx}(s-t) \\ &\quad + R_{xx}(s-t)R_{nn}(t-s) = \\ &= |F|^2 R_{xx}((1+\beta)(t-s))R_{xx}(s-t) \\ &\quad + R_{xx}(s-t)R_{nn}(t-s) = \\ &= R_{ww}(t-s) = R_{ww}(\Delta t), \end{aligned} \tag{7}$$

i.e. the process random fluctuations $w(t)$ is wide sense stationary.

By duality of multiplication in time domain and convolution in Fourier domain, the power spectral density of $w(t)$ is then

$$\begin{aligned} S_{ww}(\omega) &= \mathscr{F} R_{ww}(\Delta t) = \\ &= \left[\frac{|F|^2}{1+\beta} S_{xx}(\frac{\omega'}{(1+\beta)}) \circledast S_{xx}(-\omega') \right](\omega) \\ &\quad + \left[S_{xx}(-\omega') \circledast S_{nn}(\omega') \right](\omega) \end{aligned} \tag{8}$$

where $\circledast$ denotes the convolution. This equation is schematically illustrated on Fig. 2, where it was assumed that both $x(t)$ and $n(t)$ have rectangular power spectral densities with bandwidth B and $\beta = 0.05$. Note however that typical order of β is much smaller, $\beta \in [10^{-7}\text{–}10^{-5}]$. The high value of β improves clarity of Fig. 2, but produces the false impression that the power spectral density of $w(t)$ decreases significantly with the velocity increasing.

The first component of the sum is centred around $\omega_0\beta/(1+\beta) \approxeq \omega_0\beta$, the same as (5). The second component, focused around DC, will additionally contaminate the output of the lowpass filter $G(j\omega)$. Notice that even when the power of measurement noise $v(t)$ is 0, the 'noise floor' exists in Fourier domain due to stochastic nature of $x(t)$.

3.2 Properties of the smoothed correlation signal

Similar to above, the signal after the filter can be decomposed into expectance and residual fluctuations

$$\tilde{c}_D(t) = s(t) + z(t) \ .$$

The signal $s(t)$ is simply

$$s(t) = g(t) \circledast \mathrm{E[c_D(t)]} \tag{9}$$

where $g(t) = \mathscr{F}^{-1}G(j\omega)$ is the impulse response of the filter and, again, $\circledast$ denotes the convolution.

Similarly, the power spectral density of stochastic fluctuations $z(t)$ at the output of the filter is

$$S_{zz}(\omega) = |G(j\omega)|^2 S_{ww}(\omega) \ , \tag{10}$$

or in terms of the correlation function

$$R_{zz}(\Delta t) = g(\Delta t) \circledast R_{ww}(\Delta t) \circledast g^*(-\Delta t) \ . \tag{11}$$

Remark 1

In essence, (A3) allowed us to assume that the complex reflection coefficient F does not depend on the frequency. Note that (A3) does not in fact exclude the ultrawideband signals; the signal is considered ultrawideband when its fractional bandwidth B/F_0 exceeds 20% or when its bandwidth B exceeds 500 MHz [14]. Such 'ultrawideband but relatively narrowband' radars are described in [15].

Remark 2

Equations (9)-(11) fully describe first and second-order properties of the correlator's output. In this remark we provide the reader with some convenient approximations.

Equation (9) can be approximated as

$$s(t) \approx G(j\omega_0\beta)\mathrm{E[c(t - gd(\omega_0\beta))]}$$

where

$$\mathrm{gd}(\omega) = -\frac{\partial G(\omega)}{\partial \omega}$$

is the group delay of the filter. The approximation is valid if (A3) holds.

Similarly, since the bandwidth of $w(t)$, is many orders greater than passband of $G(j\omega)$ (c.f. (8)), (10) can be approximated as

$$S_{zz}(\omega) \approx |G(j\omega)|^2 S_{ww}(0)$$

When power spectral densities of $x(t)$ and $n(t)$ are rectangular it is straightforward to check that

$$S_{ww}(0) \approx \frac{|R_{xx}(0)|^2 + R_{xx}(0)R_{nn}(0)}{B} = R_{ww}(0)/B$$

It follows the variance of $z(t)$ can be approximately evaluated with

$$R_{zz}(0) \approx R_{ww}(0)|G(0)|^2 \frac{B_f}{B}$$

where B_f is the bandwidth of the filter $G(j\omega)$.

4 Approximate Cramér-Rao bound

We are now ready to derive the approximate Cramér-Rao bound on the accuracy of estimation of velocity v. Our derivation will be performed indirectly. Initially, the bound on more convenient quantity $\beta = 2v/c$ will be derived, which will later be used to obtain bound on v itself.

First of all, notice that the raw product $c_D(t)$ is not Gaussian. However, the smoothed correlation signal $\tilde{c}_D(t)$ has almost normal distribution[16]. We will employ this fact in our analysis. For short discussion about the accuracy of Gaussian approximation, see remark 1 at the end of the section.

For the sake of brevity, assume

(**A4**) The delay D introduced in the delay line equals to $\tau(0)$; delay introduced by the lowpass filter is negligible; the reflection coefficient $F = 1$.

Let $\mathbf{s_N}$ be a vector of $2N + 1$ samples of the expected output of the lowpass filter

$$\mathbf{s_N}_{(k)} = s(kT_s), \quad k = -N, -N+1, \cdots, N-1, N.$$

where T_s is the sampling period of lowpass filter output. Similarly, we introduce the vector of observed data

$\mathbf{c_N}$

$$\mathbf{c_{N}}_{(k)} = \tilde{c}_D(kT_s), \quad k = -N, -N+1, \cdots, N-1, N$$

and the vector of fluctuations at the output of the filter

$$\mathbf{z_N} = \mathbf{c_N} - \mathbf{s_N}.$$

The lower bound on the covariance of any unbiased estimator $\widehat{\theta}$ of unknown parameter vector θ is determined by the celebrated Cramér-Rao inequality:

$$\mathrm{E}[(\widehat{\theta} - \theta)(\widehat{\theta} - \theta)^H] \geq \mathbf{F} = \left(\mathrm{E}\left[\frac{\partial^2 \ln L}{\partial \theta \partial \theta^H} \right] \right)^{-1}$$

where A^H denotes the Herimitian transpose of A, $\mathbf{F}$ is the Fisher information matrix, L denotes the likelihood function $L(x, \theta) = p(x|\theta)$ and the averaging is performed on all possible realisations of observed data. Since however, we seek the bound on only one variable, the matrix $\mathbf{F}$ reduces to the scalar F.

The expression for Fisher's information of $2N + 1$ samples is [17]

$$F_N = 2(\frac{\partial \mathbf{s_N}}{\partial \beta})^H \mathbf{C}^{-1} (\frac{\partial \mathbf{s_N}}{\partial \beta}) + \mathrm{tr}(\mathbf{C}^{-1} \frac{\partial \mathbf{C}}{\partial \beta} \mathbf{C}^{-1} \frac{\partial \mathbf{C}}{\partial \beta}) \tag{12}$$

where $\mathbf{C}$ is the covariance matrix

$$\mathbf{C}_{(m,n)} = R_{zz}((m-n)T_s) \ .$$

Evaluating the derivatives one obtains

$$\begin{aligned} \frac{\partial s(t)}{\partial \beta} &= \frac{\partial}{\partial \beta}(g(t) \circledast R_{xx}(\beta t)) = \\ &= g(t) \circledast [R'_{xx}(\beta t) t] \\ \frac{\partial R_{zz}(\tau)}{\partial \beta} &= \left(g(\tau) \circledast \frac{\partial R_{ww}(\tau)}{\partial \beta} \circledast g^*(-\tau) \right)(\tau) \end{aligned}$$

Using above two equations, the Fisher's information and the Crámer-Rao bound can be calculated for any particular case of signal spectral densities and filter's response. However, it is rather hard (if possible at all) to arrive at any general result without further approximations and assumptions.

To cope with that issue we will once again employ (A3). It is then easy to show that

$$R'_{xx}(t) \approxeq R_{xx}(t) j\omega_0$$

because the envelope $|R_{xx}(t)|$ changes slowly compared to $e^{j\omega_0}$. It follows that

$$\frac{\partial s(t)}{\partial \beta} \approxeq G(j\omega_0\beta) R_{xx}(\beta t) j\omega_0 t = s(t) j\omega_0 t. \tag{13}$$

For the same reason (c.f. (7))

$$\frac{\partial R_{ww}(\Delta t)}{\partial \beta} \approxeq |F|^2 R_{xx}((1+\beta)\Delta t) R_{xx}(-\Delta t) j\omega_0 \Delta t \ . \tag{14}$$

To simplify matters more, we will assume that the matrix $\mathbf{C}$ is diagonal (see remark 2) and that $\partial \mathbf{C}/\partial\beta \approx 0$. This greatly simplifies the quadratic form and makes the trace term negligible, leading to

$$F_N = \frac{2}{\sigma_z^2} \sum_{k=-N}^{+N} |s(kT_s) kT_s \omega_0|^2, \tag{15}$$
$$\mathrm{Var}_N[\widehat{\beta}] \geq F_N^{-1} \ .$$

Taking the limit of (15) for $N \to \infty$ we obtain Fisher's information of infinite number of samples

$$F_\infty = \frac{2}{\sigma_z^2} \sum_{k=-\infty}^{+\infty} |s(kT_s) kT_s \omega_0|^2$$
$$\mathrm{Var}_\infty[\widehat{\beta}] \geq F_\infty^{-1} \ .$$

Introducing the quantities

$$\alpha^2 = \frac{\sum_{k=-\infty}^{+\infty} |s(kT_s) kT_s \omega_0|^2}{\sum_{k=-\infty}^{+\infty} |s(kT_s)|^2}$$
$$E = \sum_{k=-\infty}^{+\infty} |s(kT_s)|^2$$

we arrive at

$$\mathrm{Var}_\infty[\hat{\beta}] \geq \frac{1}{2(E/\sigma_z^2)\alpha^2} \ . \tag{16}$$

Finally, exploiting the fact that $\beta = 2v/c$, one can obtain the bound on the velocity itself

$$\mathrm{Var}_\infty[\hat{v}] \geq \frac{c^2}{8(E/\sigma_z^2)\alpha^2} \ . \tag{17}$$

which closely resembles a discrete-time version of the well known result for pulse radars[18].

Having derived (17) we can formulate some conclusions of qualitative nature:

1. $s(t)$ is the equivalent of the pulse envelope. Since it is a filtered version of time-stretched autocorrelation function of noise signal, its shape is determined by spectral properties of the noise signal and the frequency response of the lowpass filter.

2. The main lobe of $s(t)$ narrows as the velocity increases (this is simply a mathematical way of expressing the fact the target is leaving the range cell faster), less high power samples of $s(t)$ can be gathered and the accuracy of Doppler measurement decreases correspondingly. This is shown on fig. 3 which plots the mean square errors (17) for a range of velocities against $(2N+1)T_s$. The configuration is as follows: $B = 100$ MHz (rectangular PSD), $F_0 = 10$ GHz, $\sigma_n/\sigma_x = 1$, $B_f = 10$ kHz (ideal lowpass filter), $T_s = 1/B_f$.

3. When $|R_{xx}(\tau)|^2$ vanishes no faster than $1/\tau^3$, $F_\infty = \infty$, i.e. arbitrarily low errors can be achieved provided that the observation time is long enough. This can also be seen on Fig 3.

4. The Cramér-Rao bound is affected by velocity only little when considering short time observations, i.e. when the target does not change it's position much within the measurement. Indeed for small N, $|s(t)| \approx |s(0)|$ and the information F_N is approximately

$$\begin{aligned} F_N &= \frac{2}{\sigma_z^2} \sum_{k=-N}^{+N} |s(kT_s) kT_s \omega_0|^2 \\ &\approxeq 2\ SNR_f \sum_{k=-N}^{+N} |kT_s\omega_0|^2 \end{aligned}$$

where $SNR_f = |s(0)|^2/\sigma_z^2$ is the signal to noise ratio at the output of the lowpass filter. Therefore

$$\mathrm{Var}_N[\hat{\beta}] \geq \frac{1}{2\ SNR_f \sum_{k=-N}^{+N} |kT_s\omega_0|^2}$$

and

$$\mathrm{Var}_N[\hat{v}] \geq \frac{c^2}{8\ SNR_f \sum_{k=-N}^{+N} |kT_s\omega_0|^2}\ . \tag{18}$$

This result stresses the importance of high signal to noise ratio at the output of correlator in Doppler estimation.

5. The relative accuracy Var $\hat{\mathrm{v}}/\mathrm{v}^2$ depends on velocity for short observations , but for longer ones it gradually becomes independent (Fig. 4).

6. σ_z^2 is the variance at the output of correlator and consist of two factors: measurement noise and noise signal induced fluctuations. Therefore, even in noise-free case the accuracy of measurement is limited.

7. It is worth to compare (18) with some 'natural' bounds on accuracy. When using filterbank to perform estimation, obvious limitation is the bandwidth of the filters, which is roughly proportional to the reciprocal of the measurement time

$$\Delta f = \frac{1}{(2N+1)T_s}\ .$$

Since

$$\Delta f = \frac{2\Delta v}{c}\frac{\omega_0}{2\pi} = \frac{\Delta v \omega_0}{c\pi}$$

it follows that

$$\Delta v = \frac{c\pi}{(2N+1)T_s\omega_0}\ . \tag{19}$$

To allow fair comparison, we take square root of (18) which leads to the bound on standard deviation of measurement

$$\sigma_v \geq \frac{c}{2\sqrt{2\ SNR_f}\ \sqrt{\sum_{k=-N}^{+N} |k|^2}\ T_s\omega_0}\ .$$

The comparison with (19) once again shows the importance of high-quality signal at the output of the correlator. When SNR_f is high, it is the bandwidth of the filters that will limit the precision. On the other hand, when SNR_f is low, even the narrowest filterbank will not allow for precise measurement.

8. Finally, we stress the fact that derived formulas provide the limit of Doppler estimation based on observation of correlator output for single range cell. Naturally, by observing the target as it passes through adjacent range cells, one can achieve lower errors.

Remark 1

The lower the bandwidth B_f of the lowpass filter, the better the Gaussian approximation to probability density function of $z(t)$. Consider a noise radar with bandwidth $B = 100$ MHz. The approximate number of independent samples averaged in the filter is B/B_f. For $B_f = 10$ kHz, about 10000 independent samples are averaged in the filter, surely enough for the Gaussian hypothesis to be justified.

Remark 2

The matrix $\mathbf{C}$ is approximately diagonal for example if $B_f \ll B$, $T_s = 1/2B_f$, and the frequency response $|G(j\omega)|$ is close to ideal lowpass filter response.

4.1 Extension to multiple targets and presence of clutter

To cope with the presence of other targets and/or clutter it is sufficient here to say that returns from range cells other than D (the cell for which the measurement is made) add up to the noise $n(t)$. All targets are competing in terms of power against the total variance of the echo signal, which hampers the measurement accuracy, especially for weak targets. This also leads to somewhat unexpected conclusion that increasing the power of the transmit signal is unlikely to provide any significant improvement because eventually most of the total variance is from returns of the transmitted signal itself and not 'true' noise.

To cope with that issue, it may be most beneficial to utilise some clutter removal algorithm such as those described in [6, 7, 8], which should restore the performance of a noise radar to nearly that of a single-scatterer case.

5 Conclusions

Second order statistics of the output of correlator and approximate Cramér-Rao bound for the Doppler estimation accuracy were derived. The latter result was obtained for the point-scatter case and the discussion on the influence of presence of other targets and/or clutter was made. The limit on mean-squared Doppler error is affected by spectral properties of noise signal, thermal noise power, correlator lowpass filter frequency response, observation time, velocity of the target and the presence of other targets/clutter. It was shown that the random nature of transmitted signal causes fluctuations at the output of correlator which limit the accuracy even when thermal noise is not present. Finally, we argued that increasing transmitted power may not provide significant improvement in Doppler measurement when strong clutter is present and no means to remove clutter are taken.

References

[1] Lukin, K.A.: 'Radar Design Using Noise/Random Waveforms'. Proc. Int. Radar Symposium, Kraków, Poland, May 2006, pp. 355–358

[2] Dawood, M., and Narayanan, R.M.: 'Generalised wideband ambiguity function of a coherent ultrawideband random noise radar', IEE Proc. Radar, Sonar and Navigation, 2003, 150, (5), pp. 379–386

[3] Axelsson, S.R.J.: 'Generalized Ambiguity Functions for Ultra Wide Band Random Waveforms'. Proc. Int. Radar Symposium, Kraków, Poland, May 2006, pp. 561–564

[4] Garmatyuk, D.S, and Narayanan, R.M.: 'ECCM Capabilities of an Untrawideband Bandlimited Random Noise Imaging Radar', IEEE Tran. Aerospace and Electronic Systems, 2002, 38, (4), pp. 1243–1255

[5] Theron, I.P., and Walton, E.K., and Gunawan, S., and Lixin, C.: 'Ultrawide-band noise radar in the VHF/UHF band', IEEE Trans. Antennas and Propagation, 1999, 47, pp. 1080–1084

[6] Kulpa, K.S., and Czekala, Z.: 'Ground clutter suppression in noise radar'. Proc. Int. Conf. RADAR, Toulouse, France, October 2004, pp. 236

[7] Kulpa, K.S.: 'Simple Sea Clutter Canceller for Noise Radar'. Proc. Int. Radar Symposium, Kraków, Poland, May 2006, pp. 299–302

[8] Axelsson, S.R.J.: 'Improved Clutter Suppression In Random Noise Radar'. Proc. URSI Commission F Symposium on Microwave Remote Sensing of the Earth, Oceans, Ice, and Atmosphere; 2005

[9] Xiaojian, X., and Narayanan, R.M.: 'Range Sidelobe Suppression Technique for Coherent Ultra Wideband Random Noise Radar Imaging', IEEE Trans. Antennas and Propagation, 2001,49,(12), pp. 1836–1842

[10] Narayanan, R.M, and Dawood, M.: 'Doppler Estimation Using a Coherent Ultra-Wideband Random Noise Radar', IEEE Trans. Aerospace and Electronic Systems, 2000, 48, (6), pp. 868–878

[11] Dawood, M., and Narayanan, R.M.: 'Doppler Measurements Using a Coherent Ultrawideband Random Noise Radar'. Digest 1999 IEEE Antennas and Propagation Symposium, Orlando, FL; August 1999, pp. 2226–2229

[12] Li, Z., and Narayanan, R.M.: 'Doppler Visibility of Coherent Ultrawideband Random Noise Radar Systems', IEEE Trans. Aerospace and Electronic Systems, 2006, 42, (3), pp. 904–916

[13] Haykin, S.: 'Adaptive Filter Theory' (Prentice Hall, 2001).

[14] FCC (GPO) Title 47, Section 15 of the Code of Federal Regulations SubPart F: Ultra-wideband;.

[15] Lukin, K.A.: 'Developments of noise radar technology in LNDES IRE NASU'. Proc. of the First International Workshop on the Noise Radar Technology, Yalta, Ukraine, September 2002, pp. 90–96

[16] Dawood, M., and Narayanan, R.M.: 'Receiver Operating Characteristics for the Coherent UWB Random Noise Radar', IEEE Trans. Aerospace and Electronic Systems, 2001, 37, (2), pp. 586–594

[17] Kay, S.M.: 'Fundamentals of Statistical Signal Processing – Estimiation Theory'(Prentice Hall, 1993)

[18] Skolnik, M.I.: 'Introduction to Radar Systems.' (McGraw-Hill, 3rd ed. 2002)

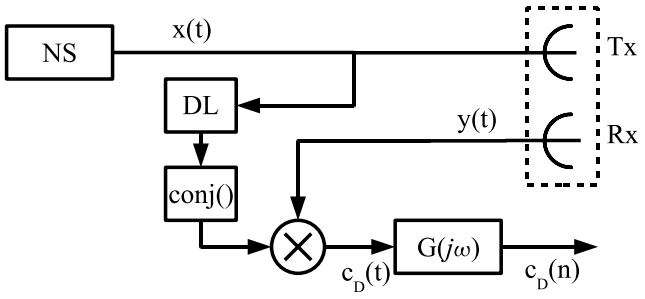

Figure 1: Block diagram of mathematical model of coherent noise radar

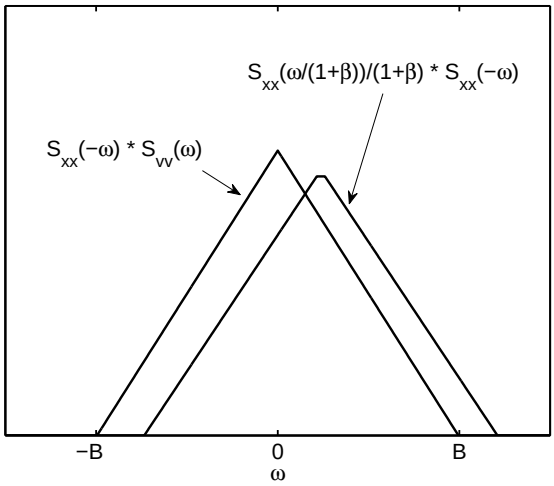

Figure 2: Two components of power spectral density of fluctuations at the output of the correlation receiver. It was assumed that both the noise signal $x(t)$ and measurement noise $n(t)$ have rectangular power spectral densities with bandwidth B and $\beta = 0.05$.

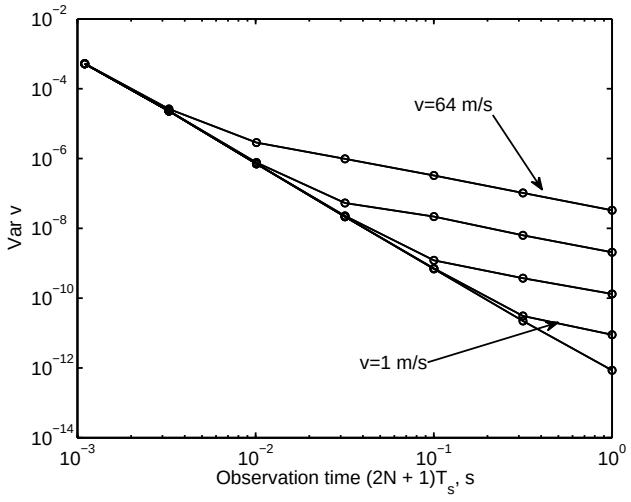

Figure 3: Mean squared errors for $v = 1, 4, 16, 64$ m/s and different observation intervals.

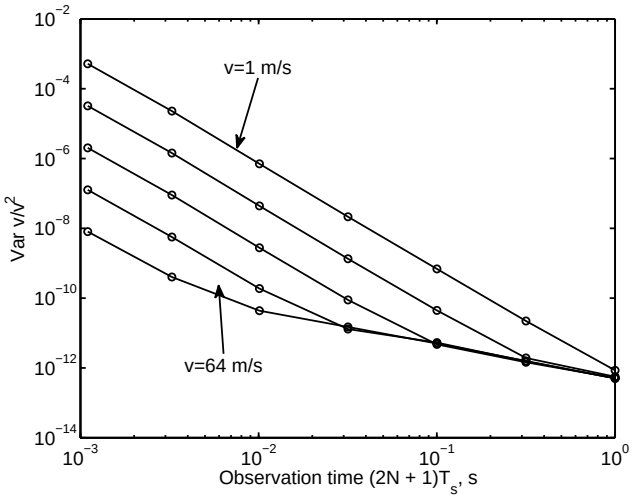

Figure 4: Relative mean squared errors for $v = 1, 4, 16, 64$ m/s and different observation intervals.